

Europium abundances in F and G disk dwarfs ^{★ ★★}

Andreas Koch and Bengt Edvardsson

Uppsala Astronomical Observatory, Box 515, SE-751 20 Uppsala, Sweden

Received 27 March 2001 / Accepted 15 October 2001

Abstract. Europium abundances for 74 F and G dwarf stars of the galactic disk have been determined from the 4129.7 Å Eu II line. The stars were selected from the sample of Edvardsson et al. (1993) and [Eu/Fe] shows a smaller scatter and a slightly weaker trend with [Fe/H] than found by Woolf et al. (1995). The data of the two analyses are homogenized and merged. We also discuss the adopted effective temperature scale.

Key words. Stars: abundances – Galaxy: abundances

1. Introduction

The study of the evolution of the Galaxy and the sites for the production of chemical elements requires observational data of the gradual changes in chemical composition of the interstellar medium as a function of time and position in the Galaxy. Slightly evolved, solar-type stars are very useful for this purpose, see e.g. the review by McWilliam (1997). Here we study europium, which is a readily observable representative of the so-called *r*-process elements. These are heavy elements formed by the *rapid* capture of neutrons on seed nuclei (much more frequent than the β -decay lifetimes). Proposed sites of the *r* process are quickly evolving core-collapse SNe and neutron star-neutron star mergers (see e.g. Thielemann et al. 2001, and references therein). These are the sites where neutron density and temperature are thought to be sufficiently high to maintain *r* processes.

Edvardsson et al. (1993, hereafter EAGLNT) investigated the abundances of 13 chemical elements in 189 disk dwarf stars with well-determined ages and galactic orbits. No *r*-process element was, however, investigated in that study. The most readily measurable such element in solar-type stars is europium through the 4129 Å Eu II line. 94% of the europium in the Sun is thought to have been produced in the *r* process. Woolf et al. (1995, WTL below) determined abundances of Eu for a northern sub-sample of the EAGLNT stars. Here their investigation is supplemented by Eu abundances for 74 southern stars of the EAGLNT sample.

In section 2 we present the observations and data reductions, section 3 gives details of the abundance analysis, while section 4 discusses the uncertainties in the results, and motivates our use of the EAGLNT effective temperature scale. Finally, sections 5 and 6 give our results and conclusions.

2. Observations and reductions

2.1. The observations

During 19 usable nights in 1994 and 1995 high-resolution spectra of 74 galactic disk F and G dwarfs were obtained. The stars were selected from the programme stars of EAGLNT. They cover a range in declination of $-65^\circ \leq \delta \leq +23^\circ$ thus giving a good addition to – and some overlap with – the northern sample of WTL. The metallicities [Fe/H] range from -1.06 to 0.26 and they have a distribution in mean galactocentric radius $5.88 \leq R_m \leq 10.10$ kpc, reflecting different sites of star formation. In the first observational period in July 1994 a spectrum of the solar disk-integrated flux was also taken. For the analysis, the Eu II line at 4129.7 Å was chosen. Among the Eu lines in the visible spectral range it is the least blended, and its strength is favourable for abundance determination.

The observations themselves were carried out at the European South Observatory (ESO) at La Silla, Chile, by means of the 1.4m Coudé Auxiliary Telescope. A wavelength region of 36 Å centered at the Eu II line at 4130 Å was observed using the Coudé Echelle Spectrograph, and the ESO CCD detectors #30 (in 1994, Ford Aerospace FA 2048 L) and #34 (in 1995, Loral Lo 2048). The dispersion was 0.02 Å per pixel and the spectral resolution was measured at about 90 000. Depending on weather conditions, the stellar brightnesses etc. the signal-to-noise ratio was about 50 at worst, and 340 for the best spectra. The aver-

Send offprint requests to: Bengt.Edvardsson@astro.uu.se

[★] Based on observations carried out at the European Southern Observatory, La Silla, Chile

^{★★} Tables 2 and 6 are only available in electronic form at <http://cdsweb.u-strasbg.fr/A+A.htm>

age S/N was ≈ 200 . Observed magnitudes reached down to $V = 8^m.3$.

2.2. The data reductions

The raw spectra were reduced using the ESO routines IHAP and MIDAS. An averaged bias was subtracted from each spectrum (including the calibration frames). Afterwards these were divided by flat-field frames. If any hits due to cosmic rays or radioactive decays within the detector affected the region around the Eu II line, these were filtered out. The continuum was rectified by carefully choosing several points that seemed to be free of lines. Division by a cubic spline function resulted in the final shape of the spectra. Wavelength calibration was then done with the spectrum of a thorium-argon lamp. For many stars two or more spectra were added to reach a useful S/N ratio. No differences in line-widths or any suspicion of background residuals are found when spectra of the same star obtained in the two separate observing runs are compared.

3. Analysis

To determine the europium abundance, synthesized spectra of the region around the Eu line were calculated with the model atmospheres that were already used in EAGLNT and Woolf et al. (1995, WTL). The parameters for α Cen B (HR 5460) were derived from the analyses of Smith et al. (1986) and Neuforge-Verheecke & Magain (1997): $T_{\text{eff}} = 5220$ K, $\log g = 4.47$, $\xi_t = 1.0$ km s $^{-1}$. The metallicity was adopted from α Cen A in EAGLNT.

The first step consisted of fitting a synthetic spectrum to the observed solar spectrum. A detailed atomic line list requested from the compiled VALD database (Kupka et al. 1999) was used. To give a better fit to the lines in the region the gf values of five lines (and their blends) were changed. Typical changes were of the order 0.05-0.1 dex. Table 1 displays the lines in the vicinity of our Eu II line.

Europium appears in two stable isotopes: ^{151}Eu and ^{153}Eu . The small difference leads to different term energies

and thus to an additional broadening of the line. For spectral syntheses the isotope ratio was assumed to be equal 50%/50%. Other authors report the solar isotope ratio as $N(^{153}\text{Eu})/N(^{151}\text{Eu}) = (52 \pm 6)/(48 \pm 6)$ (Hauge 1972), or 55/45 (Mashonkina & Gehren 2000) and e.g. the isotope ratio for Procyon (HR 2943, one of our programme stars) as $(35 \pm 15)/(65 \pm 15)$ (Kato 1987). Considering their uncertainties we expect no major error when assuming the 50/50 ratio.

Each isotopic line splits into 16 components due to hyperfine structure. We calculated these using data from Broström et al. (1995). The wavelengths, relative gf values and solar equivalent widths for all 32 components are listed in Table 2 (accessible in electronic form).

To improve the fits further, two 'artificial' lines were added as substitutes for unknown blends (see Table 1). The Eu line itself was not affected significantly by this. From this fit a solar europium abundance $A_{\text{Eu}} = 0.46$ was determined. This differs from the commonly accepted solar value of $A_{\text{Eu}} = 0.51$ (e.g. Anders & Grevesse 1989). The reason for this deviation is our use of a pure theoretical solar model atmosphere which is consistent with our stellar models, whereas Anders & Grevesse used the semi-empirical Holweger-Müller (1974) model. WTL derive from their fitted $\log gf$ values an even lower europium abundance of $A_{\text{Eu}} = 0.44$. This small difference is due to differences in the observations. To keep the analysis of the stellar spectra strictly differential relative to the Sun we use our determined value for the rest of this paper. Any modification of the gf value in the calculations would only lead to a systematic shift of all the resulting abundances, but would not change the trends that are to be seen later. Synthetic stellar spectra in the wavelength region between 4128 and 4131 Å were finally created using the above-determined gf values. The observed spectra were shifted in wavelength to match the wavelengths of the synthetic ones. This offered the possibility of controlling the quality of the fit at three points: With the help of the synthetic spectra the setting of the continuum was fine-tuned to the left of the Fe II line at 4128.7 Å, and, if necessary, shifted vertically. The second reference point of the continuum was to the red of the Fe I line at 4130.2 Å. Finally the Fe II line at 4128.7 Å served to find the adequate convolution profile. Gaussian and rotational profiles, representing the effects of macroturbulence, rotation and the instrumental profile, were thus convolved with the synthetic spectra until the iron line was well fitted in shape and depth. This line gave in general the best fit in this region since it is neither blended nor affected by atomic splitting. The 4129.4 Å Fe I line seems to contain an unknown blend in the solar spectrum which shows up also in some of the other stars, but mediocre fits of this line had no influence on the derived europium abundances.

Fig. 1 shows some of the observed spectra together with the fitted synthetic spectra. The highly broadened lines of the hotter or fast rotating stars gave rise to higher uncertainties on the abundances, since several lines overlap there and form one broad feature. The wings widen

Table 1. The most dominant lines in the synthesized region of the solar spectrum

Wavelength [Å]	Origin	$\log gf$	Equivalent width [mÅ]
4128.748	Fe II	-3.830	43.3
4129.159	Ti II	-2.330	25.4
4129.166	Ti I	0.131	32.1
4129.196	Cr I	-1.374	10.8
4129.220	Fe I	-2.280	35.3
4129.461	Fe I	-2.160	42.3
4129.530	'Fake' (Fe I)	-3.355	10.5
4129.725	Eu II	0.173	31.7
4129.965	'Fake' (Fe I)	-3.455	19.5
4130.037	Fe I	-4.280	24.5
4130.038	Fe I	-2.470	40.4

to such a large extent that the continuum is not reached, which made its setting more difficult and sensitive to possible inadequacies in the line data. Nonetheless the routine of abundance determination was the same as for the less broadened, clear line spectra.

The result of our analysis are logarithmic europium abundances relative to hydrogen normalized on the Sun, $[\text{Eu}/\text{H}]_{\text{II}}^1$.

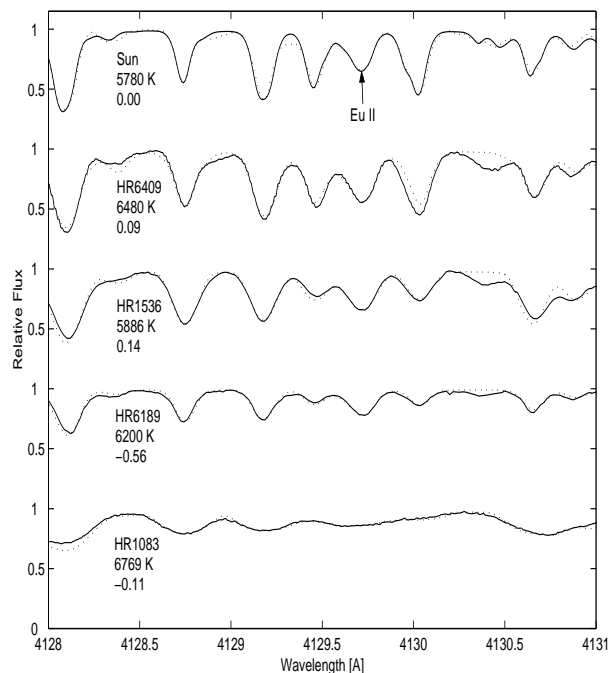


Fig. 1. Sample observed spectra (solid lines), the dotted lines show the synthetic spectra; the feature at 4130 Å a blend of Gd II and Ni I, was neglected in the fit. Given are also the effective temperatures and overall metallicities

4. Error estimates and previous data

4.1. Errors in the models

One error source in these abundance determinations is the adopted model atmospheres, either by uncertain parameters used there or by the simplifying assumptions that were made (LTE, plane parallel atmospheres etc.). Over the years the MARCS (Gustafsson et al. 1975) model atmospheres were improved, primarily by updates of the opacities. The effects of these changes are small: models calculated in the year 2000 give europium abundances lower by 0.01 dex on average than the older ones from 1993 used by EAGLNT and WTL.

In general model atmospheres may have errors in the fundamental parameters. The influence of these error sources on abundances is discussed at large in EAGLNT. In that paper it is argued that no uncertainty in temperature larger than 100 K should occur, which followed from

¹ $[\text{Eu}/\text{H}]_{\text{II}} = \log \frac{(N_{\text{Eu}}/N_{\text{H}})_{\star}}{(N_{\text{Eu}}/N_{\text{H}})_{\odot}}$, measured from the Eu II line.

error estimates of the basic photometric ($b - y$) data; the analogous estimate for gravity is 0.2 dex in $\log g$.

The models and the photometric effective temperature scale derived by EAGLNT have, however, been challenged. Blackwell et al. (1995) studied the limb darkening properties of three solar models: the semiempirical Holweger & Müller (1974, HM) model, the theoretical flux-constant model of Kurucz (1992, K92) and the theoretical flux-constant model presented in EAGLNT and used here. The T vs. τ relation of the HM model was constructed "by hand" to fit the profiles of strong spectral lines and the solar limb darkening and therefore it has a different temperature structure as compared the flux-constant theoretical models. It thus fits the observed solar limb darkening quite well, at the cost of not being flux-constant. The EAGLNT and Kurucz models are both theoretical, using the mixing-length approximation for convective energy transport. The K92 solar model also introduced an "approximate overshooting" scheme on top of the mixing-length scheme in order to decrease the temperature gradient. This brought the model to show a limb darkening which is approximately half way between the HM and the EAGLNT models. The behaviour of this approximate overshooting recipe for other stars than the Sun was discussed by Castelli, Gratton & Kurucz (1997). They showed that the approximate overshooting scheme can not simultaneously fit the Sun and other solar-type stars, and this option has been abandoned in later versions of the K92 model atmospheres programme. The problem seems to be essentially absent in 3-dimensional hydrodynamic solar model atmospheres (Asplund et al. 1999). In our differential analysis the aim is to circumvent systematic errors by application of the same (non-perfect) analysis to the target stars as to the reference star, in this case the Sun.

Also the effective temperature scale of EAGLNT has been questioned. Gratton et al. (1996) used the infrared flux method and interferometric diameters and the the K92 models with approximate overshooting to establish an effective temperature scale, which deviates strongly from the EAGLNT scale as a function of metallicity (see their Fig. 10). It is not clear to us whether this large systematic difference may be caused by the use of the approximate overshooting recipe which they later abandoned (see above). A metallicity dependent variation of the T_{eff} scale of EAGLNT by 250 K would have introduced unacceptable deviations from excitation equilibrium in their sample (EAGLNT Sect. 4.3.4), and very severe line-to-line scatter in the derived chemical abundances.

Alonso et al. (1994) used JHK photometry to determine effective temperatures for 550 late-type dwarf and sub-giant stars. 31 of their stars overlap with the sample of EAGLNT, and the mean difference Alonso et al. minus EAGLNT is -50 K and a scatter of ± 80 K, without any obvious trends with T_{eff} , $\log g$ or $[\text{Fe}/\text{H}]$.

Gratton et al. (1996) also used the effective-temperature sensitive H_{α} line profiles as support for their temperature scale calibration. Hydrogen line-profile cal-

culations have also been used for T_{eff} calibrations by e.g. Fuhrmann et al. (1993, 1994) and Gardiner et al. (1999). Barklem et al. (2000, 2001), however, show that the hydrogen line-broadening theory used in these and previous calculations has substantial systematic errors which vary with metallicity and effective temperature. This is due to the neglect of hydrogen self-broadening. In particular, previous balmer line calibration work has overestimated the effective temperatures for cool and for metal-poor stars (Barklem et al. 2000).

Gustafsson (1997) also discussed in more detail the reliability and use of model atmospheres.

These considerations and also the small sensitivity to model parameter errors of the abundance results discussed next, make us stick to the T_{eff} scale of EAGLNT. This also makes our results consistent with our previous data for the same stars.

To quantify the influence of uncertainties in the model parameters we carried out alternative model calculations for four representative stars. Table 3 displays the computed effects on the derived abundances. The average uncertainty on europium abundance when using models with $\Delta T_{\text{eff}} = +100$ K was $+0.02$ dex, whereas the models with a smaller $\log g$ diminished the europium abundances by 0.07 dex on average.

The same procedure was carried out in EAGLNT for their error estimates, and the result for $[\text{Fe}/\text{H}]_{\text{II}}$ was an error of -0.02 dex and -0.09 dex for the same changes of ΔT_{eff} and $\Delta \log g$, respectively. If we add our error estimates to those of EAGLNT we get the resulting uncertainties by model effects in the crucial quantity: $\Delta[\text{Eu}/\text{Fe}]_{\text{II}} \approx +0.04$ for temperature changes and $\Delta[\text{Eu}/\text{Fe}]_{\text{II}} \approx +0.02$ for gravity changes. EAGLNT furthermore estimates an uncertainty in the microturbulence parameter of $\pm 0.3 \text{ km s}^{-1}$. Such changes in our models gave no significant changes in europium abundances. Since EAGLNT made sure that the metallicities adopted for the models are consistent with the spectroscopic values, they should not cause any discernible error.

Recent NLTE calculations for Eu II have been carried out by Mashonkina & Gehren (2000). The slight underpopulation of the ground level and overpopulation of the excited levels do not contribute significantly to the errors, since most of the effect cancels out in our differential analysis.

Table 3. Effects on $[\text{Eu}/\text{H}]_{\text{II}}$ of model changes for typical programme stars

ID	$(T_{\text{eff}}, \log g, [\text{Fe}/\text{H}])$	ΔT_{eff}	$\Delta \log g$
		+100K	-0.2 dex
HR 1083	(6769, 4.10, -0.11)	0.00	-0.08
HR 1687	(6596, 4.15, 0.26)	0.02	-0.07
HR 4903	(5953, 4.00, 0.24)	0.03	-0.07
HD 199289	(5894, 4.38, -1.03)	0.03	-0.05

4.2. Errors in reduction and determination

Since both continuum setting and the fitting of synthetic spectra to observations is done via a fit by eye, these may be important error sources. We tested the sensitivity to a continuum uncertainty by introducing a change in the continuum setting of 2%. This typically led to abundance changes by 0.02 dex. Errors in the iron abundance due to the continuum setting are found to be negligible in EAGLNT. The fitting of the synthesized spectra to the observations was found to be a major error source for some stars. From high S/N spectra of stars with narrow lines abundances could be derived with an estimated fitting uncertainty of ± 0.01 dex. But in the case of a low S/N ratio or very broad lines this precision cannot be maintained. Here the fit was far more difficult and the uncertainties may reach ± 0.05 dex.

Spectra of the same stars that were observed during different observing runs and thus differing e.g. in S/N, were also analysed separately. These were found to give consistent abundances.

Finally all the errors listed here are added in quadrature and we find $\Delta[\text{Eu}/\text{H}]_{\text{II}} \approx \pm 0.08$ dex, $\Delta[\text{Fe}/\text{H}]_{\text{II}} \approx \pm 0.11$ (corresponding to the estimates in EAGLNT), and finally $\Delta[\text{Eu}/\text{Fe}]_{\text{II}} \approx \pm 0.05$ dex for the spectra of better quality and on the other hand $\Delta[\text{Eu}/\text{H}]_{\text{II}} \approx \pm 0.09$ dex, and $\Delta[\text{Eu}/\text{Fe}]_{\text{II}} \approx \pm 0.07$ dex for the abundances from broader lines.

4.3. Previous europium data

The first larger determination of europium abundances was released 25 years ago by Butcher (1975). In his work he included 32 galactic G dwarfs. The derived abundances contained uncertainties of about 25%. Butchers' $[\text{Eu}/\text{H}]$ results have a standard deviation of 0.13 from our data. No systematic shift with metallicity is found when Butchers' data are compared to ours.

One of the programme stars of da Silva et al. (1990) was HR 3018, which was also observed by us. They derive an abundance of $[\text{Eu}/\text{Fe}]_{\text{II}} = 0.39$, whereas we give its abundance as 0.37. The deviation is smaller than the estimated uncertainties. In general HR 3018 was the star whose abundance coincides in nearly all observational runs

Table 4. Comparison of $[\text{Eu}/\text{Fe}]_{\text{II}}$ from different projects. Not all of the WTL stars are included

ID	This paper	Woolf et al. (1995)	Zhao (1994)	Butcher (1975)
HR 1101	0.03	-0.07		-0.21
HR 2883	0.23	0.26	0.09	
HR 2943	0.02	0.02		0.04
HR 3018	0.37	0.38	0.32	0.23
HR 3578	0.44	0.47	0.42	0.32
HR 4540	0.02	-0.03		0.12
HR 8181	0.15		0.11	0.15
HD 215257	0.17			0.06

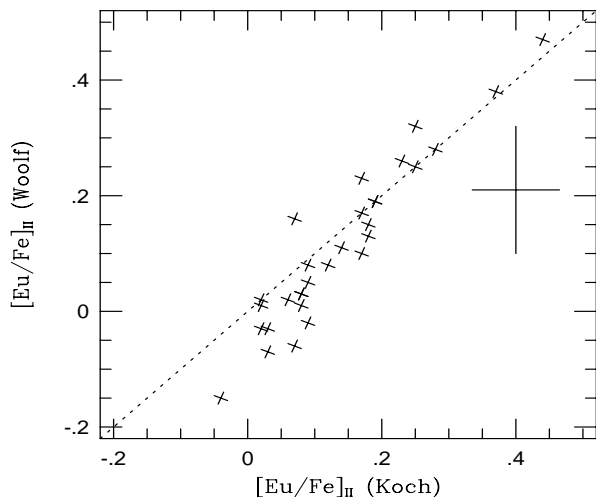


Fig. 2. Comparison of Eu abundances with Woolf et al. (1995). Error bars of the magnitudes estimated in the two investigations are plotted. The dotted line is unity

so far. Gratton & Sneden (1994) report for this star a value of 0.38, corresponding very well to our result. Their work contains furthermore our programme star HR 2883, for which they give an abundance of 0.14 ± 0.07 . This is significantly lower than our value of 0.23 ± 0.06 , but still consistent within the uncertainties. A lower abundance of 0.09 for this cool metal-poor star was derived by Zhao (1994). Other stars from Zhao’s paper correspond well with our values (see Table 4). The newer paper of Mashonkina & Gehren (2000) has 3 stars in common with our paper. One of them, HR 7560, has an abundance of -0.01 compared to our derived $[\text{Eu}/\text{Fe}]_{\text{II}} = 0.12$. If the same values of T_{eff} and $\log g$ were used, however, the abundances would be consistent within the respective uncertainties.

One of the latest and the most extensive studies of europium abundances in solar type stars was presented by WTL. It included 81 disk F and G type stars from the EAGLNT sample. They estimated uncertainties in $[\text{Eu}/\text{Fe}]_{\text{II}}$ of about 0.11 dex. 30 of their programme stars were also observed by us; the comparison in Fig. 2 shows that our derived abundances are generally slightly higher, and show a systematic trend with $[\text{Eu}/\text{Fe}]$. The error bars are misleading in this plot, however, since the iron abundances, models and model parameters of EAGLNT were used in both the investigations. The figure therefore reflects the differences in the line strengths of the Eu line between the two investigations. If the slightly different solar Eu abundances were taken into account, a systematic upward (or leftward) shift of all data points by 0.02 dex would occur. The trend implies that the ratios of our Eu line strengths to those of WTL increase with increasing metallicity. Comparisons between reduced spectra from WTL and the present paper suggest that the cause of this difference is a larger uncertainty in the continuum level near the Eu line of the WTL data, due to a considerably shorter observed spectral interval, and with an

Eu line position typically only 3.5 \AA from the red edge of the spectrum. This explanation is supported by the larger scatter in $[\text{Eu}/\text{Fe}]$ vs. $[\text{Fe}/\text{H}]$ found for the WTL data in the next section. Table 4, finally, gives a comparison for some stars analysed by different authors.

5. Results and discussion

Europium abundances of the 74 F and G stars determined during this project are listed in Table 5 (also available in electronic form). The remaining parameters are taken from EAGLNT. Their $[\text{Fe}/\text{H}]_{\text{II}}$ abundance and age for α Cen A (HR 5459) are adopted for α Cen B (HR 5460).

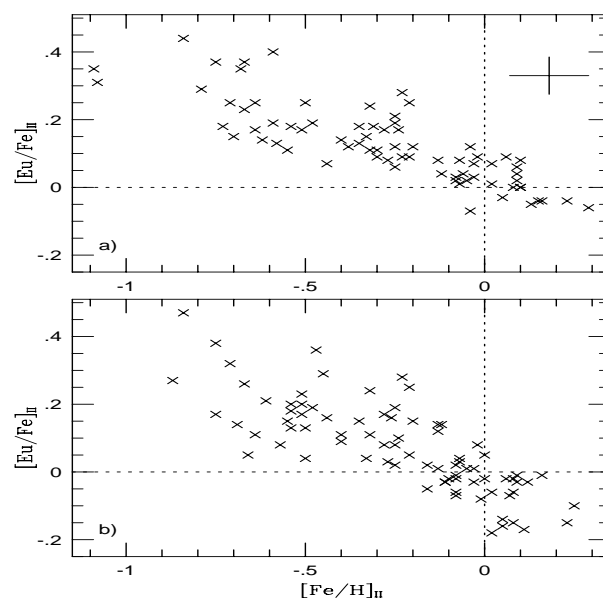


Fig. 3. Europium abundance relative to iron vs. iron. In panel a) our data is shown and the indicated error bar is of typical size. In panel b) the corresponding data of Woolf et al. (1995) is shown

Fig. 3a displays $[\text{Eu}/\text{Fe}]_{\text{II}}$ vs. $[\text{Fe}/\text{H}]_{\text{II}}$ for our data. We use the singly ionized state of both elements since these are the dominant species in the solar type stars and this ratio is only weakly dependent on surface gravities and possible overionization effects. A linear least squares fit to the data yields a slope of $\Delta[\text{Eu}/\text{Fe}]_{\text{II}}/\Delta[\text{Fe}/\text{H}]_{\text{II}} = -0.31 \pm 0.02$. At solar metallicities there is an offset in y-direction of $+0.04 \pm 0.01$. The scatter in $[\text{Eu}/\text{Fe}]_{\text{II}}$ relative to the linear fit to the diagram is 0.065 dex (s.d.). Following WTL a more quantitative approach to the scatter around the slope was obtained by means of a Monte Carlo simulation in which we calculated Gaussian distributed random pairs of iron and europium abundances. The estimates from Sect. 4 were taken as representative 1σ random errors scattering around the theoretical slope of -0.31 . The simulated scatter diagram is similar to the observed scatter. Since the scatter in our new data set is smaller than that of WTL (see below), this strengthens their conclusion that

Table 5. Derived Eu abundances. The iron abundances are from EAGLNT

ID	[Fe/H] _I	[Fe/H] _{II}	[Eu/H] _{II}	[Eu/Fe] _{II}	ID	[Fe/H] _I	[Fe/H] _{II}	[Eu/H] _{II}	[Eu/Fe] _{II}
HR 33	-0.38	-0.40	-0.26	0.14	HR 4657	-0.70	-0.71	-0.46	0.25
HR 35	-0.10	-0.12	-0.08	0.04	HR 4734	0.10	0.10	0.10	0.00
HR 107	-0.37	-0.35	-0.22	0.13	HR 4903	0.24	0.29	0.23	-0.06
HR 140	0.05	-0.04	-0.11	-0.07	HR 4989	-0.28	-0.30	-0.19	0.11
HR 235	-0.15	-0.28	-0.11	0.17	HR 5338	-0.11	-0.07	-0.06	0.01
HR 366	-0.32	-0.35	-0.17	0.18	HR 5460	0.15	0.19	0.11	-0.08
HR 368	-0.24	-0.25	-0.06	0.19	HR 5542	0.13	0.09	0.15	0.06
HR 370	0.12	0.05	0.01	-0.04	HR 5698	0.01	0.08	0.08	0.00
HR 573	-0.34	-0.30	-0.21	0.09	HR 5723	-0.13	-0.13	-0.05	0.08
HR 646	-0.32	-0.25	-0.19	0.06	HR 5996	0.23	0.16	0.12	-0.04
HR 672	0.06	-0.07	-0.01	0.08	HR 6189	-0.56	-0.59	-0.40	0.19
HR 740	-0.25	-0.27	-0.19	0.08	HR 6243	0.00	0.02	0.03	0.01
HR 1010	-0.23	-0.33	-0.18	0.15	HR 6409	0.09	0.09	0.13	0.04
HR 1083	-0.11	-0.20	-0.08	0.12	HR 6569	-0.27	-0.23	-0.14	0.09
HR 1101	-0.11	-0.08	-0.05	0.03	HR 6649	-0.32	-0.34	-0.21	0.11
HR 1173	0.09	-0.02	0.07	0.09	HR 6907	0.13	0.10	0.18	0.08
HR 1257	0.02	0.04	0.09	0.07	HR 7126	0.21	0.10	0.10	0.00
HR 1536	0.14	0.06	0.15	0.09	HR 7560	0.09	-0.04	0.08	0.12
HR 1545	-0.33	-0.51	-0.34	0.17	HR 7875	-0.44	-0.38	-0.26	0.12
HR 1673	-0.30	-0.25	-0.13	0.12	HR 8077	-0.07	-0.06	-0.02	0.04
HR 1687	0.26	0.23	0.19	-0.04	HR 8181	-0.67	-0.70	-0.55	0.15
HR 1983	-0.07	-0.03	0.00	0.03	HR 8665	-0.32	-0.21	-0.12	0.09
HR 2233	-0.17	-0.21	0.04	0.25	HR 8697	-0.25	-0.31	-0.13	0.18
HR 2354	0.13	0.13	0.08	-0.05	HR 8969	-0.17	-0.23	0.05	0.28
HR 2530	-0.43	-0.44	-0.37	0.07	HD 6434	-0.54	-0.59	-0.19	0.40
HR 2548	-0.20	-0.25	-0.04	0.21	HD 17548	-0.59	-0.62	-0.48	0.14
HR 2835	-0.55	-0.54	-0.36	0.18	HD 25704	-0.85	-0.79	-0.50	0.29
HR 2883	-0.75	-0.67	-0.44	0.23	HD 51929	-0.64	-0.68	-0.33	0.35
HR 2906	-0.18	-0.05	-0.03	0.02	HD 78747	-0.64	-0.67	-0.30	0.37
HR 2943	-0.02	-0.08	-0.06	0.02	HD 130551	-0.62	-0.58	-0.45	0.13
HR 3018	-0.78	-0.75	-0.38	0.37	HD 165401	-0.47	-0.50	-0.25	0.25
HR 3220	-0.26	-0.32	-0.08	0.24	HD 188815	-0.58	-0.55	-0.44	0.11
HR 3578	-0.82	-0.84	-0.40	0.44	HD 199289	-1.03	-1.08	-0.77	0.31
HR 4039	-0.38	-0.48	-0.29	0.19	HD 201891	-1.06	-1.09	-0.74	0.35
HR 4158	-0.24	-0.24	-0.07	0.17	HD 210752	-0.64	-0.73	-0.55	0.18
HR 4395	-0.10	-0.03	0.04	0.07	HD 215257	-0.65	-0.64	-0.47	0.17
HR 4540	0.13	0.09	0.11	0.02	HD 218504	-0.62	-0.64	-0.39	0.25

most of the scatter in the results can be explained by observational, analytical and systematic errors rather than by real stellar scatter of abundances.

Fig. 3b shows the corresponding results from WTL. Here the slope of a linear fit is -0.39 and the line passes the solar metallicity at $[\text{Eu}/\text{Fe}]_{\text{II}} = -0.02$. The scatter relative to a linear least squares fit to Fig. 3b is 0.082 dex, and their Eu abundances are lower than ours at the higher metallicities.

To homogenize and merge the data we derive a simple linear transformation between the two data sets in Fig. 3. Motivated by the smaller scatter in Fig. 3a, and the discussion in the end of Sect. 4.3, we chose to adjust the WTL data to our results and derive $\Delta[\text{Eu}/\text{H}] = [\text{Eu}/\text{H}](\text{Koch}) - [\text{Eu}/\text{H}](\text{WTL}) = 0.0619 + 0.0833[\text{Fe}/\text{H}]_{\text{II}}$. For stars observed in both analyses the weights were taken to be proportional to inverted squares of the standard deviations from the linear fits to Figs. 3a and b. This data for the 125 stars is given in Table 6 (avail-

able in electronic form), which gives $[\text{Eu}/\text{H}]_{\text{II}}$, $[\text{Fe}/\text{H}]_{\text{II}}$, $[\text{Eu}/\text{Fe}]_{\text{II}}$ and \log age for each star.

A definite trend is also present in the abundance vs. age diagram for the merged data set, Fig. 4. $[\text{Eu}/\text{Fe}]_{\text{II}}$ increases by a factor of two over the stellar age range, although both the Eu and the Fe abundances (relative to hydrogen) decrease with age. The isochronic ages were adopted from EAGLNT. Later new age data has been published by Ng & Bertelli (1998). If we plot our abundances against these new ages instead of these used in EAGLNT we find the same trend but with a larger scatter.

Our new results and Eu abundance trends are not greatly different from those of WTL. We therefore refer the reader to their discussion of the results.

6. Conclusions

The analysis of 74 F and G type galactic disk dwarfs from the sample of Edvardsson et al. (1993) shows that the abundance ratio $[\text{Eu}/\text{Fe}]_{\text{II}}$ decreases with a slope of

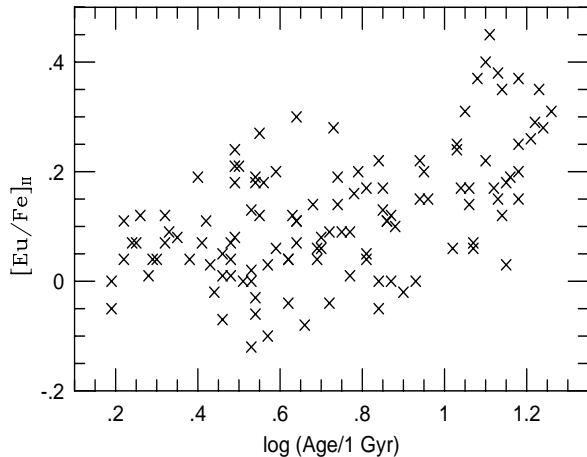


Fig. 4. $[\text{Eu}/\text{Fe}]_{\ln}$ vs. $\log \text{age}$ using our data merged with those of Woolf et al. (1995). The ages are adopted from EAGLNT

-0.31 dex/dex with increasing metallicity in the observed range $-1.06 < [\text{Fe}/\text{H}] < 0.29$. This slope is about 20% smaller than that found by Woolfe et al. (1995), and the scatter around the trend is also reduced.

Our data have been merged with those of Woolf et al. (1995), after a slight adjustment of the latter, to form a data set of 125 stars with metallicities $[\text{Fe}/\text{H}] \gtrsim -1.1$. To improve the data set needed for studies of the formation and evolution of r -process elements, more data for the low and very low metallicity range is needed.

Acknowledgements. We would like to thank Vincent Woolf for making available his data and for swift help. Bengt Gustafsson is thanked for discussions and suggestions and the anonymous referee for very helpful comments to the manuscript. We thank Anders Wännström for help and discussions of hyperfine structure calculations and Sofia Feltzing for performing parts of the observations. We acknowledge Patrik Thorén and Torgny Karlsson for help with software and discussions. BE acknowledges support from the Swedish Natural Science Research Council, NFR.

References

- Alonso A., Arribas S., Martínez-Roger C. 1994, A&AS 107, 365
 Anders E., Grevesse N. 1989, Geochim. Cosmochim. Acta 53, 197
 Asplund M., Nordlund Å, Trampedach R. 1999, ASP Conf. Ser. 173: Theory and Tests of Convection in Stellar Structure, eds. A.Giménez, E.F.Guinan, B.Montesinos, 221
 Barklem P.S., Piskunov N., O'Mara B.J. 2000, A&A 363, 1091
 Barklem P.S. et al. 2001, in preparation
 Blackwell D.E., Lynas-Gray A.E., Smith G. 1995, A&A 296, 217
 Broström L., Mannervik S., Royen P., Wännström A. 1995, Phys. Scr. 51, 330
 Butler H.R. 1975, ApJ 199, 710
 Castelli F., Gratton R.G., Kurucz R.L., 1997, A&A 318, 841

- Edvardsson B., Andersen J., Gustafsson B., Lambert D.L., Nissen P.E., Tomkin J. 1993, A&A 275, 101 (EAGLNT)
 Fuhrmann K., Axer M., Gehren T. 1993, A&A 271, 451
 Fuhrmann K., Axer M., Gehren T. 1994, A&A 285, 585
 Gardiner R.B., Kupka F., Smalley B. 1999, A&A 347, 876
 Elements, ed. Prantzos, Cassé & Vangioni-Flam, 492
 Gratton R.G., Carretta E., Castelli F. 1996, A&A 314, 191
 Gratton R.G., Sneden C. 1994, A&A 287, 927
 Gustafsson B. 1997, in IAU Symp. 189, Fundamental Stellar Properties: The Interaction between Observation and Theory, eds. T.R.Bedding et al., 261
 Gustafsson B., Bell R.A., Eriksson K. Nordlund Å. 1975, A&A 42, 407
 Hauge Ø. 1972, Sol. Phys. 27, 286
 Holweger H., Müller E.A. 1974, Sol. Phys. 39, 19 (HM)
 Kato K. 1987, Publ. Astron. Soc. Japan 39, 517
 Kupka F., Piskunov N.E., Ryabchikova T.A., Stempels H.C., Weiss W.W. 1999, A&AS 138, 119
 Kurucz R.L. 1992, Rev. Mex. Astron. Astrofis. 23, 181 (K92)
 Mashonkina L., Gehren T. 2000, A&A 364, 249
 McWilliam A. 1997, ARA&A 35, 503
 Neuforge-Verheecke C., Magain P. 1997, A&A 328, 261
 Ng Y.K., Bertelli G. 1998, A&A 329, 943
 da Silva L., da la Reza R., de Magalhães S.D. 1990, in Astrophysical Ages and Dating Methods, 5th IAP Workshop, ed. Vangioni-Flam, 419
 Smith G., Edvardsson B., Frisk U. 1986, A&A 165, 126
 Thielemann F.-K., Brachwitz F., Freiburghaus C. et al. 2001, Prog. Nucl. Part. Phys., preprint (astro-ph/0101476)
 Woolf V.M., Tomkin J., Lambert D.L. 1995, ApJ 453, 660 (WTL)
 Zhao G. 1994, Chin. Astron. Astrophys 18, 85